



BCL-B (BCL2L10) is overexpressed in patients suffering from multiple myeloma (MM) and drives an MM-like disease in transgenic mice

Mohamed Amine Hamouda, Arnaud Jacquel, Guillaume Robert, Alexandre Puissant, Valentine Richez, Roméo Cassel, Nina Fenouille, Sandrine Roulland, Jérôme Gilleron, Emmanuel Griessinger, et al.

► To cite this version:

Mohamed Amine Hamouda, Arnaud Jacquel, Guillaume Robert, Alexandre Puissant, Valentine Richez, et al.. BCL-B (BCL2L10) is overexpressed in patients suffering from multiple myeloma (MM) and drives an MM-like disease in transgenic mice. *Journal of Experimental Medicine*, 2016, [Epub ahead of print]. 10.1084/jem.20150983 . inserm-01353362

HAL Id: inserm-01353362

<https://www.hal.inserm.fr/inserm-01353362>

Submitted on 11 Aug 2016

HAL is a multi-disciplinary open access archive for the deposit and dissemination of scientific research documents, whether they are published or not. The documents may come from teaching and research institutions in France or abroad, or from public or private research centers.

L'archive ouverte pluridisciplinaire **HAL**, est destinée au dépôt et à la diffusion de documents scientifiques de niveau recherche, publiés ou non, émanant des établissements d'enseignement et de recherche français ou étrangers, des laboratoires publics ou privés.

BCL-B (BCL2L10) is overexpressed in patients suffering from multiple myeloma (MM) and drives an MM-like disease in transgenic mice

Mohamed-Amine Hamouda,^{1,6,7} Arnaud Jacquel,^{1,6,7} Guillaume Robert,^{1,6,7} Alexandre Puissant,^{8,9} Valentine Richez,^{1,17} Romeo Cassel,^{1,6,7} Nina Fenouille,¹⁰ Sandrine Roulland,¹¹ Jerome Gilleron,^{2,6} Emmanuel Griessinger,^{3,6} Alix Dubois,^{1,6,7} Beatrice Bailly-Maitre,^{4,6} Diogo Goncalves,^{1,6,7} Aude Mallavialle,^{5,6} Pascal Colosetti,^{1,6,7} Sandrine Marchetti,^{1,6,7} Martine Amiot,¹² Patricia Gomez-Bougie,¹² Nathalie Rochet,^{6,13} Marcel Deckert,^{5,6} Herve Avet-Loiseau,¹⁴ Paul Hofman,¹⁵ Jean-Michel Karsenti,¹⁶ Pierre-Yves Jeandel,¹⁷ Claudine Blin-Wakkach,^{6,18} Bertrand Nadel,¹¹ Thomas Cluzeau,^{1,6,7,16} Kenneth C. Anderson,^{8,9} Jean-Gabriel Fuzibet,¹⁷ Patrick Auberger,^{1,6,7*} and Frederic Luciano^{1,6,7*}

¹Team 2, ²Team 7, ³Team 4, ⁴Team 8, and ⁵Team 11, Institut National de la Santé et de la Recherche Médicale (INSERM) U1065, Centre Méditerranéen de Médecine Moléculaire (C3M), 06204 Nice, France

⁶Université de Nice Sophia-Antipolis, 06000 Nice, France

⁷Equipe Labellisée par la Ligue Nationale Contre le Cancer, 75013 Paris, France

⁸Dana-Farber Cancer Institute and ⁹Boston Children's Hospital, Harvard Medical School, Boston, MA 02115

¹⁰Koch Institute for Integrative Cancer Research, Massachusetts Institute of Technology, Cambridge, MA 02142

¹¹Centre d'Immunologie de Marseille-Luminy, Aix-Marseille University, INSERM U1104, Centre National de la Recherche Scientifique (CNRS) UMR 7280, 13288 Marseille, France

¹²Team 10, INSERM U892, 44007 Nantes, France

¹³UMR 7277, 06108 Nice, France

¹⁴Cancer Research Center of Toulouse, UMR 1037, INSERM-Université Toulouse III Paul Sabatier (UPS)-CNRS, 31037 Toulouse, France

¹⁵Service d'Anatomopathologie, ¹⁶Service d'Hématologie Clinique, and ¹⁷Service de Médecine Interne, Centre Hospitalier Universitaire de Nice, 06003 Nice, France

¹⁸CNRS UMR 7370, 06108 Nice, France

Multiple myeloma (MM) evolves from a premalignant condition known as monoclonal gammopathy of undetermined significance (MGUS). However, the factors underlying the malignant transformation of plasmacytes in MM are not fully characterized. We report here that $\text{E}\mu$ -directed expression of the antiapoptotic Bcl-B protein in mice drives an MM phenotype that reproduces accurately the human disease. Indeed, with age, $\text{E}\mu$ -bcl-b transgenic mice develop the characteristic features of human MM, including bone malignant plasma cell infiltration, a monoclonal immunoglobulin peak, immunoglobulin deposit in renal tubules, and highly characteristic bone lytic lesions. In addition, the tumors are serially transplantable in irradiated wild-type mice, underlying the tumoral origin of the disease. $\text{E}\mu$ -bcl-b plasmacytes show increased expression of a panel of genes known to be dysregulated in human MM pathogenesis. Treatment of $\text{E}\mu$ -bcl-b mice with drugs currently used to treat patients such as melphalan and VELCADE efficiently kills malignant plasmacytes in vivo. Finally, we find that Bcl-B is overexpressed in plasmacytes from MM patients but neither in MGUS patients nor in healthy individuals, suggesting that Bcl-B may drive MM. These findings suggest that Bcl-B could be an important factor in MM disease and pinpoint $\text{E}\mu$ -bcl-b mice as a pertinent model to validate new therapies in MM.

INTRODUCTION

Multiple myeloma (MM) is a malignant condition that evolves from monoclonal gammopathy of undetermined significance (MGUS) and corresponds to the expansion of abnormal plas-

macytes in the BM (Palumbo and Anderson, 2011). Autologous stem cell transplantation remains a good option for treating this disease; however, all patients will unavoidably relapse. Therefore, considerable efforts have been devoted to the development of new therapeutic options for the treatment of patients suffering from MM. Although drugs such as lenalid-

*P. Auberger and F. Luciano contributed equally to this paper.

Correspondence to Frederic Luciano: fluciano@unice.fr

Abbreviations used: MGUS, monoclonal gammopathy of undetermined significance; MM, multiple myeloma; M-spike, monoclonal spike; PC, plasma cell; SHM, somatic hypermutation; SPEP, serum protein electrophoresis; TRAP, tartrate-resistant acid phosphatase.

© 2016 Hamouda et al. This article is distributed under the terms of an Attribution-Noncommercial-Share Alike-No Mirror Sites license for the first six months after the publication date (see <http://www.rupress.org/terms>). After six months it is available under a Creative Commons License (Attribution-Noncommercial-Share Alike 3.0 Unported license, as described at <http://creativecommons.org/licenses/by-nc-sa/3.0/>).

omide (REVLIMID) and bortezomib (VELCADE) have significantly improved the overall survival rates of patients, MM remains an incurable disease, and there is an urgent need for new therapies (Strobeck, 2007; Ludwig et al., 2010).

Among the six human antiapoptotic Bcl-2 family proteins (Bcl-2 [BCL2], Bcl-X_L [BCL2L1], Mcl-1 [MCL1], Bcl-W [BCL2L2], Bfl-1 [BCL2A1], and Bcl-B [BCL2L10]; Adams and Cory, 1998), Bcl-B was the last antiapoptotic member to be identified, and its physiological function is only partially understood (Ke et al., 2001; Zhai et al., 2003). Bcl-B is expressed predominantly in normal human B lymphocytes and is pathologically overexpressed in malignant plasma cells (PCs) and many types of solid tumors such as prostate, mammary, colorectal, and lung carcinomas (Luciano et al., 2007; Krajewska et al., 2008). Mice lack the *bcl-b* gene; however, the closest homologue (Diva/Boo) is predominantly expressed in ovary and testis and exhibits a proapoptotic rather than an antiapoptotic phenotype (Inohara et al., 1998).

Pangenomic studies have been extensively used to isolate genes that are differentially expressed in PCs from healthy donors versus MGUS and MM patients (Claudio et al., 2002; Davies et al., 2003; De Vos et al., 2003; Carrasco et al., 2006). None of these studies identified the *bcl-b* gene as a candidate promoting the genesis and progression of MM. However, a recent report showed that ubiquitination and proteasomal turnover dictate the expression level of the Bcl-B protein and thereby its antiapoptotic activity (Beverly et al., 2012; van de Kooij et al., 2013; Rooswinkel et al., 2014). Consequently, determination of the Bcl-B protein level appears to be the only reliable approach for evaluating its oncogenic potential.

The generation of specific mouse models of MM is not only an important challenge but also a prerequisite for better characterization and understanding of the molecular mechanisms involved in MM pathogenesis and the progression from MGUS to MM. In addition, the availability of mouse models that accurately recapitulate MM could be of considerable interest for the validation of new therapeutic strategies for this disease. However, attempts to develop such models (3'KE-*bcl-x_L*, *Igh-c-myc* Eμ-*c-maf*) have generally yielded B cell malignancies displaying immature phenotypes or plasmacytomas rather than MM (Linden et al., 2004; Park et al., 2005; Morito et al., 2011). Several other animal models of MM (Eμ-*xbp-1s*, 3'KE-*bcl-x_L*/Eμ-*c-myc*, *bcl-x_L* × *imyc*) have been reported but do not recapitulate all of the characteristics of human MM from the clinical, pathological, and genetic points of view (Cheung et al., 2004; Boylan et al., 2007; Carrasco et al., 2007). Only the vk**myc* mouse model, in which the activation of *c-myc* oncogene occurs sporadically through the physiological somatic hypermutation (SHM) process, fulfills most of the biological and genetic criteria of an ideal mouse model of MM (Chesi et al., 2008).

In the present study, we identify the pathophysiological function of Bcl-B for the first time. Of note, we show that specific overexpression of Bcl-B in the B cell compartment drives an MM-like disease in transgenic mice that recapitulates

the main features of the human pathology, including a unique IgG monoclonal peak driven by specific immunoglobulin rearrangements, PC infiltration in the BM, anemia, lytic bone lesions, and kidney immunoglobulin deposits. Unlike previously characterized MM mouse models, in which penetrance was relatively low, 100% of Eμ-*bcl-b* mice develop the disease. In addition, Eμ-*bcl-b* mice exhibit increased expression of proteins involved in the regulation of B cell proliferation and plasmacyte differentiation, including *Xbp-1s*.

The discovery that Bcl-B could be an important factor in PC homeostasis that can drive an MM-like disease in mice may have important clinical implications.

RESULTS

Bcl-B is predominantly expressed in the BM of MM patients

We previously reported Bcl-B overexpression in histological BM sections from MM patients (Luciano et al., 2007; Krajewska et al., 2008). To confirm Bcl-B protein expression, we used a dedicated flow cytometry assay (Cluzeau et al., 2012). Fig. 1 A shows an example of Bcl-B protein expression measurement by flow cytometry in an MGUS patient and an MM patient with 3.6% and 28.2% of medullar plasmocytes, respectively. We found that most of the plasmocytes from the MM patient highly expressed the Bcl-B protein, whereas a negligible proportion of the plasmocytes from the MGUS patient weakly expressed the Bcl-B protein. In patients with newly diagnosed MM (*n* = 18), 20–100% of sorted CD138⁺ BM cells were positive for Bcl-B, whereas only a very small percentage (0–10%) of CD138⁺ BM cells from healthy donors (*n* = 3) and MGUS patients (*n* = 20) were positive for this protein (Fig. 1 B). The level of Bcl-B expression was next analyzed by Western blot using plasmocytes from two healthy donors, three MGUS patients, and eight patients with newly diagnosed MM. All MM patients expressed Bcl-B, whereas the protein was almost undetectable in healthy donors and MGUS patients (Fig. 1 C). We finally examined different MM cell lines for the expression of Bcl-B, Bcl-2, and Mcl-1 because these two latter Bcl-2 family members were previously reported to be important for MM pathogenesis (Spets et al., 2002; Gomez-Bougie et al., 2004; Wuillème-Toumi et al., 2005; Morales et al., 2011). The level of Bcl-B expression was homogeneous in all of the MM cell lines, whereas significant variation was observed for Bcl-2 and Mcl-1 expression from one cell line to another (Fig. 1, D and E, top). In the corresponding MM cell lines, we also examined the expression of Bcl-B at the RNA level. Although there was not a perfect correlation between the mRNA level and the protein expression, amplification of Bcl-B mRNA was observed in most cell lines (Fig. 1, D and E, bottom). We also detected homogeneous expression of Bcl-B in all B cell lymphoma cell lines tested that was equivalent in intensity to that detected in MM. Interestingly, the Bcl-B protein was not detected in two myeloid cell lines (not depicted).

These results are in agreement with previous studies that have demonstrated that the expression level of Bcl-B

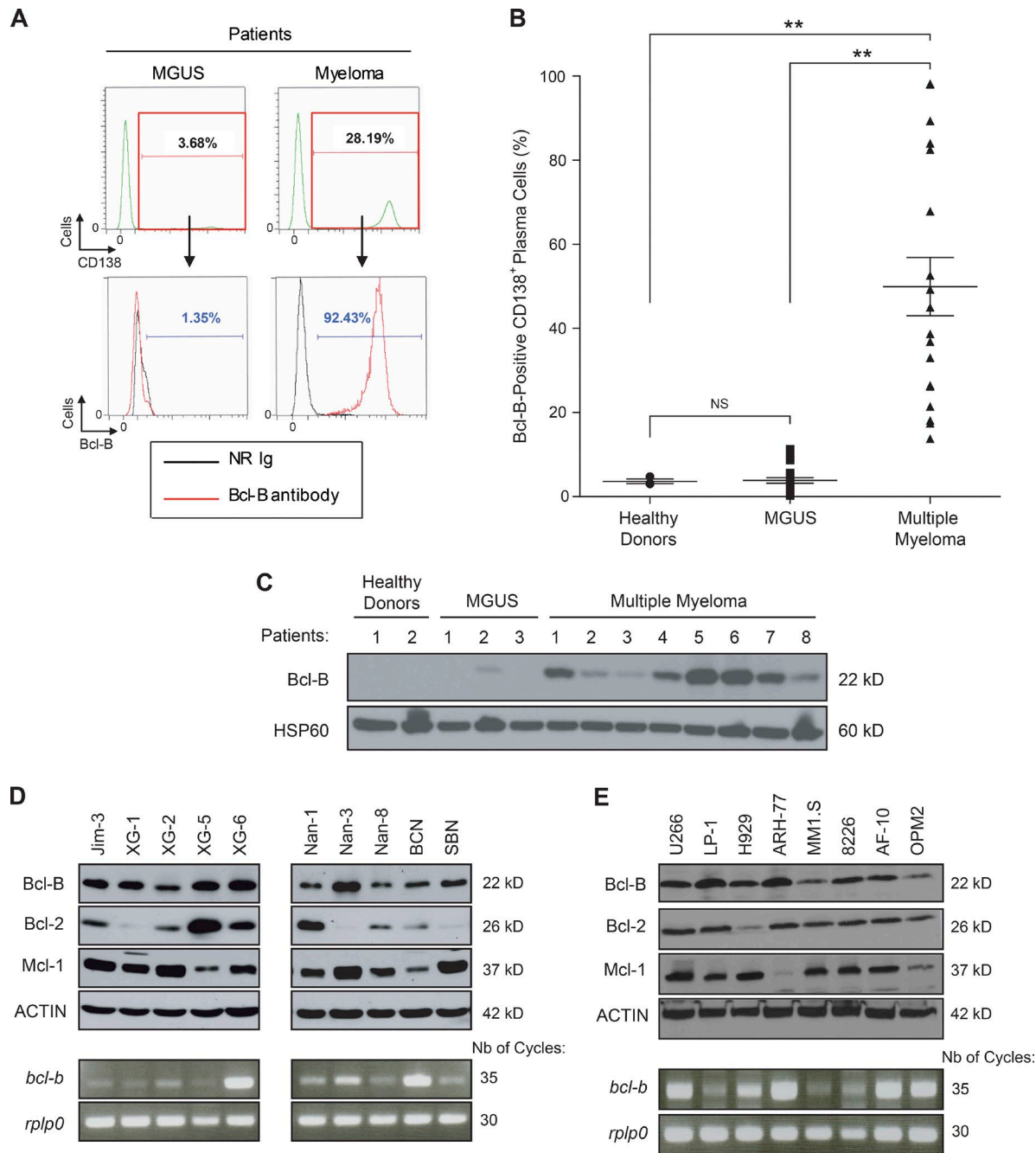


Figure 1. Bcl-B protein is predominantly expressed in the BM of patients suffering from MM and is widely expressed in human MM cell lines. (A) Representative cytometric profiles as examples of Bcl-B-positive PC quantification by flow cytometry analysis of BM cells from an MGUS and an MM patient. Total BM cells were quantified, and Bcl-B protein expression was measured by gating the CD138-positive fraction corresponding to medullar plasmacytes. NR Ig, nonrelevant rabbit Ig. (B) The percentage of Bcl-B-positive PCs was quantified by flow cytometry analysis of BM cells from healthy donors ($n = 3$), MGUS patients ($n = 20$), and patients with newly diagnosed MM ($n = 18$). P-values were determined by one-way ANOVA. NS, no significant difference was observed. **, $P < 0.01$. Results are expressed as the mean \pm SD. (C) PCs were isolated from the BM of healthy donors (lanes 1 and 2), MGUS patients (lanes 3–5), and MM patients (lanes 6–13) using CD138 magnetic beads. Total protein lysates (35 μ g per lane) were subjected to Western blot analysis using anti-Bcl-B or Hsp60 antibodies. (D and E) Total protein extracts (30 μ g) from a panel of human MM cell lines were subjected to SDS-PAGE/immunoblot using Bcl-B, Bcl-2, Mcl-1, and Actin antibodies (top). In parallel, *bcl-b* transcript level was determined by RT-PCR (bottom).

protein is mainly dependent on its posttranscriptional regulation and that the abundance of the transcript does not reflect the expression level of the protein (Beverly et al., 2012; van de Kooij et al., 2013; Rooswinkel et al., 2014). Collectively, these data suggest that Bcl-B protein could be a robust marker of MM disease.

Expression of Bcl-B in B cells drives MM in transgenic mice

To investigate the role of Bcl-B in plasmacyte homeostasis, we designed transgenic mice carrying the Bcl-B open reading frame under the control of the immunoglobulin VH promoter and E μ enhancer elements (E μ -bcl-b mice; Fig. 2 A). Among the eight founders obtained, we further analyzed those expressing the transgene exclusively in B cells. All of them developed an MM-like disease. We further focused on the founder line with intermediate expression of Bcl-B. As expected, the E μ regulatory elements specifically drove expression of Bcl-B only in the BM, spleen, and lymph nodes (Fig. 2 B). Although endogenous Bcl-B protein is absent in mice, the functionality of exogenous Bcl-B protein was confirmed in splenic cells isolated from E μ -bcl-b mice based on its ability to interact with the BH3-only family member Bim (not depicted).

The overall survival of homozygous (+/+) E μ -bcl-b mice (Fig. 2 C, red curve) was significantly lower than that of control mice (Fig. 2 C, black curve). Half of the homozygous (+/+) E μ -bcl-b mice died within 18 mo versus 26 mo for the control mice. Moreover, all (+/+) E μ -bcl-b mice were dead at 20 mo compared with only 10% of the control mice. Of note, hemizygous (-/+) E μ -bcl-b mice showed an intermediate overall survival that correlated with the twofold lower Bcl-B expression in the corresponding plasmacytes (Fig. 2 C, blue curve and inset). For the rest of the study, we used almost exclusively hemizygous (-/+) E μ -bcl-b mice. With age, E μ -bcl-b mice exhibited an increased proportion of CD138⁺ plasmacytes in their BM (Fig. 2 D). The increased proportion of CD138⁺ plasmacytes was also confirmed by immunofluorescence and by May-Grünwald-Giemsa (MGG) staining (not depicted). At 15 mo, the mean percentage of mature plasmacytes (B220⁻/CD138⁺) was 15.58% (with a range of 5% to 52%) in E μ -bcl-b mice versus only 0.47% in control mice. Importantly, neither WT nor transgenic young mice developed plasmacytosis (not depicted). As is the case for MM patients who often develop anemia, E μ -bcl-b mice exhibited reduced hemoglobin levels (mean = 7.5 g/dl, *n* = 28) compared with their control counterparts (mean = 13.2 g/dl, *n* = 16; Fig. 2 E). Although all aged Bcl-B mice developed an MM-like disease, the incidence of the splenomegaly in E μ -bcl-b mice was only 53.3% (not depicted). Splenomegaly was accompanied by an increase in cellularity and a significant increase in mature B cell number. However, we failed to detect any increase in CD138-positive cells, corresponding to plasmacytes, in the spleens of E μ -bcl-b mice. At the same time, we identified a comparable proportion of T cells, B cells, and PCs in the lymph nodes of wild-type and E μ -bcl-b mice (not

depicted). Moreover, E μ -bcl-b mice exhibited characteristic lytic bone lesions (Fig. 2 F, top) compared with their control counterparts (Fig. 2 F, top). Indeed, areas of bone destruction were clearly visible in E μ -bcl-b mice (Fig. 2 F, yellow arrows). Tartrate-resistant acid phosphatase (TRAP) staining was also analyzed in the trabecular zone of the femurs from WT and E μ -bcl-b transgenic mice. The black arrows indicate significantly more TRAP-positive osteoclasts (purple staining) in E μ -bcl-b mice. Images were analyzed to define the areas corresponding to TRAP staining. These areas were normalized to the bone areas and revealed a significant increase in TRAP-positive cells in E μ -bcl-b mice compared with WT mice (not depicted). Congo red staining of histochemical sections from the kidneys of wild-type and E μ -bcl-b mice showed reddish and intense orange deposits in the latter, corresponding to amyloid deposition (Fig. 2 G, left). This was confirmed under polarized light (Fig. 2 G, right). The bright green is the “apple green birefringence” that is characteristic of amyloid deposition. Such deposits are also reminiscent of the human pathology.

E μ -bcl-b mice exhibit monoclonal hypergammaglobulinemia

Serum protein electrophoresis (SPEP) on the blood of 18-month-old mice confirmed the diagnosis of myeloma (Fig. 3 A). The presence of a monoclonal spike (M-spike; γ -globulin peak) in transgenic mice is indicated by an arrow (Fig. 3 A). A prominent γ -globulin peak was also detected in the sera of 9 out of 11 mice, and a fainter one was present in the 2 remaining mice (Fig. 3 B). We also analyzed the appearance of the γ -globulin peak in the serum of transgenic mice as a function of the disease progression (Fig. 3 C). The immunoglobulin peak was faintly detected at 12 mo and was maximal after 18 mo of age, but undetectable in the serum of 24-month-old control mice (Fig. 3 C). Densitometric analysis showed a time-dependent increase of gammaglobulinemia in the serum of four transgenic mice and a parallel decrease in albumin production (Fig. 3 D). The decrease in serum albumin level is a hallmark of human MM that was reported in the previously generated MM mouse model (Chesi et al., 2008). A selective increase in IgG2b was detected by ELISA in the sera of homozygous E μ -bcl-b (*n* = 30) versus control mice (*n* = 15), whereas no increase in the IgG1 and IgG3 levels was noted (Fig. 3 E). IgA and IgM levels were significantly decreased in homozygous E μ -bcl-b mice. This finding is in agreement with the situation observed in the human disease. Globally, from this data, we concluded that 86.7% of the homozygous E μ -bcl-b mice developed a monoclonal gammopathy. In comparison, 38.1% of the hemizygous transgenic mice developed a monoclonal gammopathy (not depicted). To further confirm the monoclonal origin of the tumors that developed in the E μ -bcl-b transgenic mice, we analyzed immunoglobulin heavy and light chain gene rearrangements in sorted CD138⁺ plasmacytes from two WT and three E μ -bcl-b mice (compare Table S3). PCR analysis revealed the clonal origin of the tumor in homozygous transgenic mouse #1 for both IgH

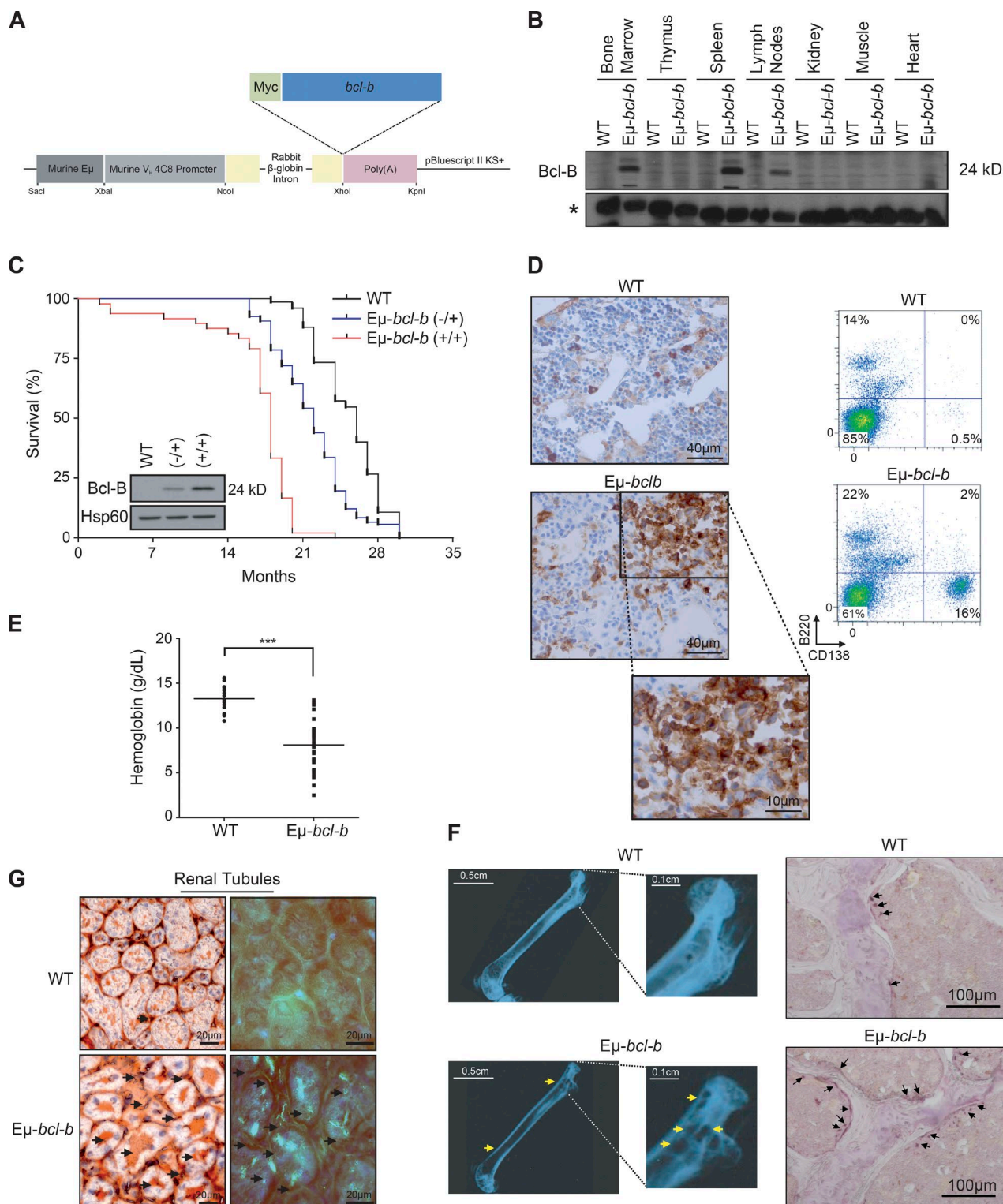


Figure 2. Generation and characterization of Eμ-*bcl-b* transgenic mice. (A) Transgenic mice were designed that carry the Myc-*bcl-b* open reading frame under the control of the immunoglobulin VH promoter and Eμ enhancer elements (Eμ-*bcl-b* mice). (B) The Bcl-B protein level was analyzed by Western blot in the spleen, lymph node, thymus, BM, kidney, muscle, and heart of 8-wk-old control or Eμ-*bcl-b* transgenic mice. The asterisk indicates a nonspecific band used as a loading control. (C) The graph represents the overall survival (in months) of a cohort of 56 WT, 80 hemizygous (-/+), and 48 homozygous (+/+) Eμ-*bcl-b* mice. Statistically significant differences ($P < 0.005$) were detected between Eμ-*bcl-b* transgenic and control littermates. (inset) Splenic cells from WT, (-/+), and (+/+) Eμ-*bcl-b* mice were collected and lysed, and the total protein extracts were subjected to SDS-PAGE/

and Igk, with five identical clones out of five sequenced in each case. Regarding the second transgenic mouse (tumor #2), which was also supposed to be homozygous, the results for the monoclonality on the basis of the IgK locus appear very clear, whereas the results for the monoclonality on the basis of the IgH locus, where a dominant B cell clone population represents at least 50% of the myeloma cells, appear less clear. Therefore, one can consider mouse #2 as oligoclonal. Globally, there was good evidence of clonal expansion for both mouse #1 and #2 compared with WT mice. In contrast, for the third transgenic mouse (tumor #3), which was known to be hemizygous, the tumor was clearly polyclonal. This was not unexpected because two-thirds of the hemizygous $E\mu$ -*bcl-b* transgenic mice produce more than one monoclonal antibody. Finally, sequence analysis of the VDJH4 and VKJK variable regions showed evidence of SHM and intraclonal diversity accumulation, both compatible with a clonal expansion process. In conclusion, despite the low number of mice tested, a monoclonal origin was established for the two homozygous $E\mu$ -*bcl-b* mouse tumors. Collectively, the results from Fig. 3 and Table S3 confirm the monoclonality of the disease.

Set of genes modulated in $E\mu$ -*bcl-b* plasmacytes

To compare gene expression profiles of control and $E\mu$ -*bcl-b* mice, we performed dedicated microarrays covering the main cytokines affected in MM and important cellular pathways involved in B cell proliferation and differentiation. We observed a significant increase in the mRNA expression of key factors involved in the pathogenesis of human MM, including *igf-1*, *il-6*, and *il-7* cytokines; *c-myc*, *ccnd2*, *c-maf*, and *c-jun* proto-oncogenes; and *irf-4*, *prdm-1*, and *xbp-1* key genes involved in B cell and plasmacyte differentiation (Iida et al., 1997; Borson et al., 2002; Klein et al., 2003; Shaffer et al., 2008; Ohguchi et al., 2016). Of note, modulation of mRNA expression of the bone resorption factors *rank*, *rank-l*, *bmp-6*, and *trap* was also detected (Fig. 4). Collectively, this pattern of mRNA expression is in agreement with the MM phenotype developed by the $E\mu$ -*bcl-b* mice.

The malignant PCs of $E\mu$ -*bcl-b* mice are serially transplantable and are sensitive to conventional MM therapies

To determine whether the BM cells from $E\mu$ -*bcl-b* mice have the potential to generate clinical features of MM into sec-

ondary recipients, BM mononuclear cells from transgenic and control mice were i.v. injected into lethally irradiated syngeneic C57BL/6 mice. Conversely to mice transplanted with control BM cells, those transplanted with transgenic BM cells showed signs of weakness after 2 mo. The $CD138^+$ /B220⁻ PC expansion was maintained in the BM of the first and second transplants (Fig. 5 A), and SPEP analysis detected a monoclonal peak in the sera of transplanted mice (Fig. 5 B). Blood analysis also revealed a drastic reduction in hemoglobin and hematocrit levels (Fig. 5 C). Mice serially transplanted with control BM cells had no evidence of plasmacytosis, IgG peak, or blood count anomalies. The clonogenic potential of BM cells from $E\mu$ -*bcl-b* or wild-type secondary transplanted mice was further analyzed. Only BM cells from $E\mu$ -*bcl-b* mice harbored a high clonogenic potential and could be expanded in culture medium supplemented with mouse-ril-7 (Fig. 5, D–F). Indeed, after 14 d, the proportion of B220⁺/CD138⁺ PCs in the BM of $E\mu$ -*bcl-b* mice drastically increased (Fig. 5 G). All together, these findings confirm the tumorigenic nature of the $E\mu$ -*bcl-b* mice plasmacytes.

To determine whether the $E\mu$ -*bcl-b* are sensitive to conventional chemotherapies, 24-mo-old transgenic and control mice were treated with either VELCADE (0.5 mg/kg twice a week for 6 wk) or melphalan (1.25 mg/kg once a day for 5 wk; Fig. 5 H). At the end of both treatments, a drastic diminution of the plasmacytosis in the BM from the transgenic mice was observed. In parallel, we showed that the B (B220⁺), T (CD4⁺/CD8⁺), and monogranulocytic (GR1⁺) populations were not affected by both treatments in BM or spleen from control or transgenic mice (not depicted). These results show that the tumorigenic plasmacytes from the $E\mu$ -*bcl-b* mice are sensitive to conventional therapies and confirm that our model could be used to test innovative therapeutic strategies.

Increased plasmocyte proliferation and differentiation of $E\mu$ -*bcl-b* splenic B cells

We next investigated the role of Bcl-B in B cell proliferation and plasmocyte differentiation ex vivo. Splenic B cells from 8-wk-old control and $E\mu$ -*bcl-b* mice were incubated ex vivo with LPS. LPS significantly increased the number of B cells in wild-type mice at 3 d (Fig. 6 A). Splenic B cells isolated from Bcl-B mice exhibited a 2.5-fold increase in B cell number in response to LPS, whereas non-B cells were unaffected (Fig. 6, A and B). During plasmocyte differentia-

immunoblot using Bcl-B and Hsp60 antibodies. (D, left) PCs from BM sections of hemizygous 18-mo-old WT or $E\mu$ -*bcl-b* mice were stained with an anti-CD138 antibody. (right) The infiltration of PCs into the BM of transgenic mice was confirmed by flow cytometry using B220 and CD138 antibodies. (E) Hemoglobin levels in the peripheral blood were measured in 18-mo-old WT mice ($n = 16$) and $E\mu$ -*bcl-b* mice ($n = 28$). ***, $P < 0.0001$ using a two-tailed Student's *t* test for unpaired data. Horizontal bars indicate median. (F, left) Freshly isolated nondecalcified femurs from WT and hemizygous $E\mu$ -*bcl-b* transgenic mice were x-rayed. The yellow arrows indicate lytic bone lesions in $E\mu$ -*bcl-b* mice. (right) TRAP staining was analyzed in the trabecular zone of the femurs from WT and $E\mu$ -*bcl-b* transgenic mice. The black arrows indicate more TRAP-positive osteoclasts (purple color) in $E\mu$ -*bcl-b* mice. (G) Renal tissue sections from 18-mo-old control (WT) and hemizygous $E\mu$ -*bcl-b* mice were stained with Congo red. (left) Sections were mounted, and brightfield images were acquired. The black arrows indicate amyloid deposition in the interstitium. (right) Polarized images were also acquired. The bright green is the "apple green birefringence" that is characteristic of amyloid.

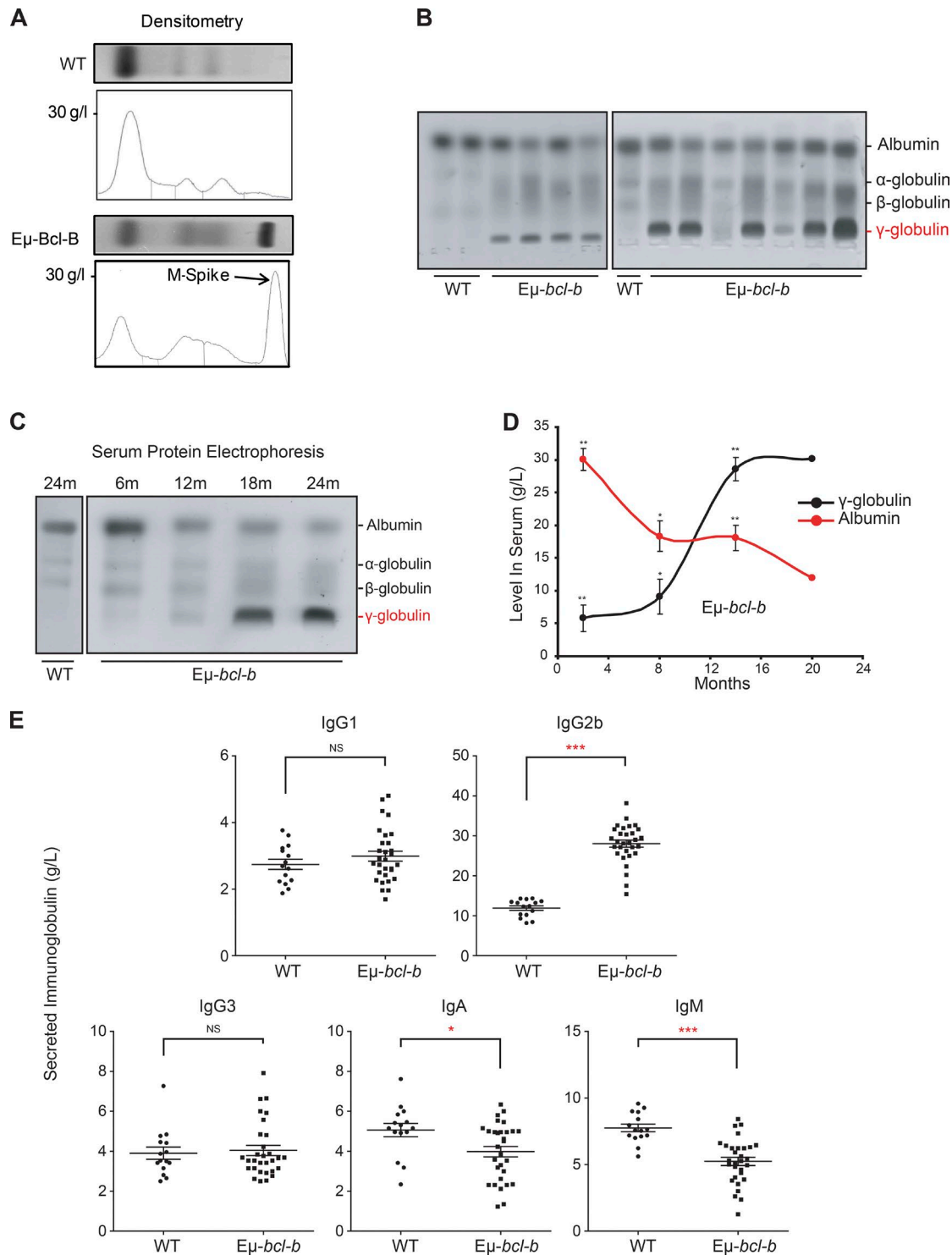


Figure 3. **Eμ-bcl-b transgenic mice exhibit monoclonal gammopathy.** (A) SPEP was performed with the sera of representative 18-mo-old WT and hemizygous Eμ-bcl-b mice. The presence of an M-spike (γ-globulin peak) in the transgenic mice is indicated by an arrow. (B) SPEP was performed with the sera of 18-mo-old mice (3 control and 11 hemizygous Eμ-bcl-b transgenic mice). The positions of albumin and the different globulins are indicated. (C) SPEP was performed on WT and hemizygous Eμ-bcl-b mice at the indicated age (months). The positions of albumin and the different globulins are indicated. (D) Densitometric analysis of albumin and γ-globulin in the sera of four Eμ-bcl-b mice was performed. Note the hypergammaglobulinemia and hypoalbuminemia in hemizygous Eμ-bcl-b mice. (E) Sera from 18-mo-old WT ($n = 15$) or homozygous Eμ-bcl-b ($n = 30$) mice were analyzed by ELISA. ***, $P < 0.001$; **, $P < 0.01$; *, $P < 0.05$ using a two-tailed Student's t test for unpaired data. Results are expressed as the mean \pm SD.

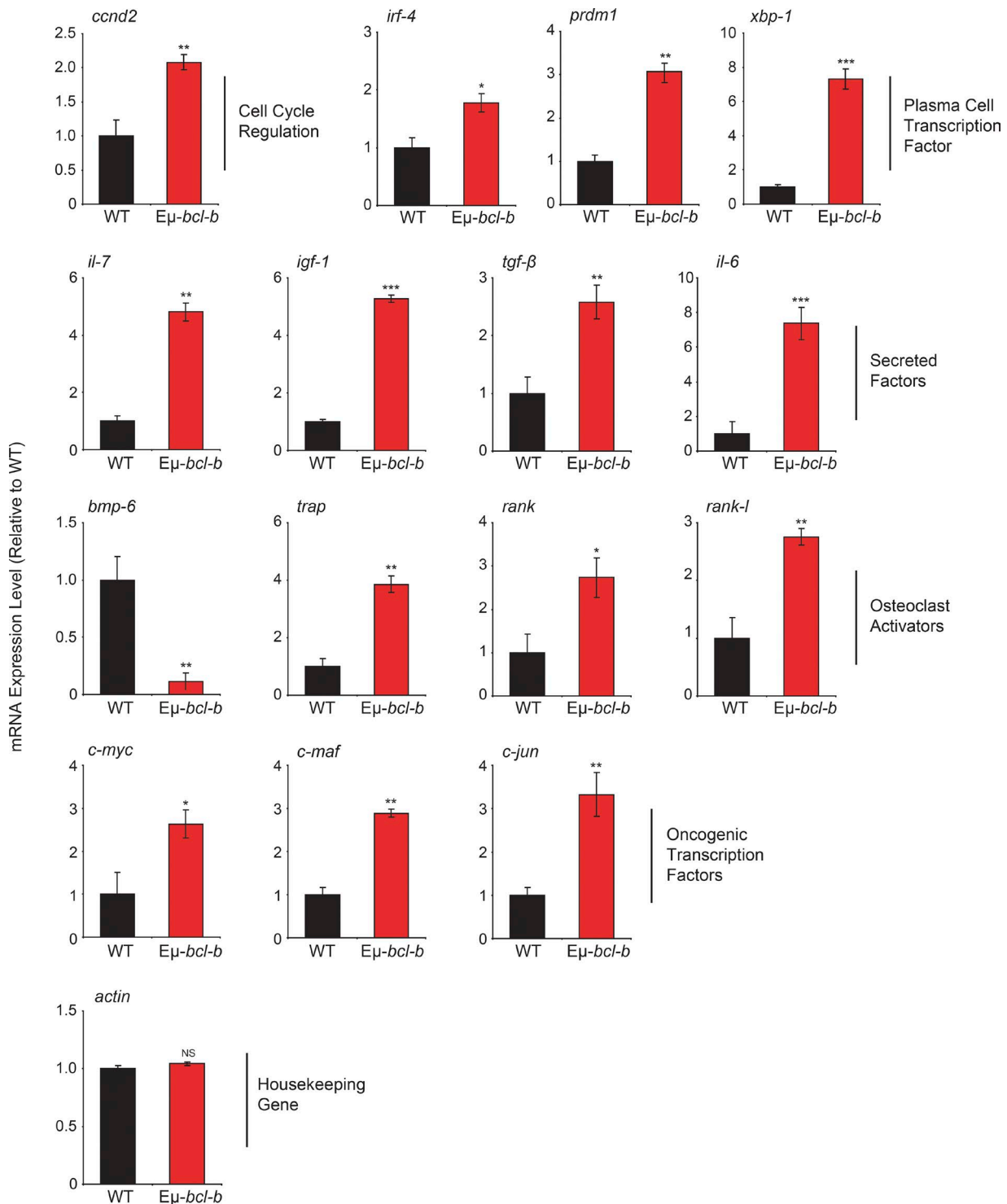


Figure 4. **Eμ-bcl-b mice exhibit an mRNA expression pattern that is compatible with the MM phenotype.** Total RNA was obtained from sorted medullar plasmacytes of 18-mo-old control WT mice ($n = 4$) and transgenic hemizygous Eμ-bcl-b developing myeloma ($n = 4$) mice. The mRNA expression levels of genes implicated in growth, PC differentiation, and bone resorption were analyzed by quantitative RT-PCR. The expression levels were normalized accordingly to the ubiquitin and β-actin housekeeping genes. Where indicated, the cumulative data \pm SD from independent experiments are shown. ***, $P < 0.001$; **, $P < 0.005$; *, $P < 0.05$, using a two-tailed Student's t test for unpaired data.

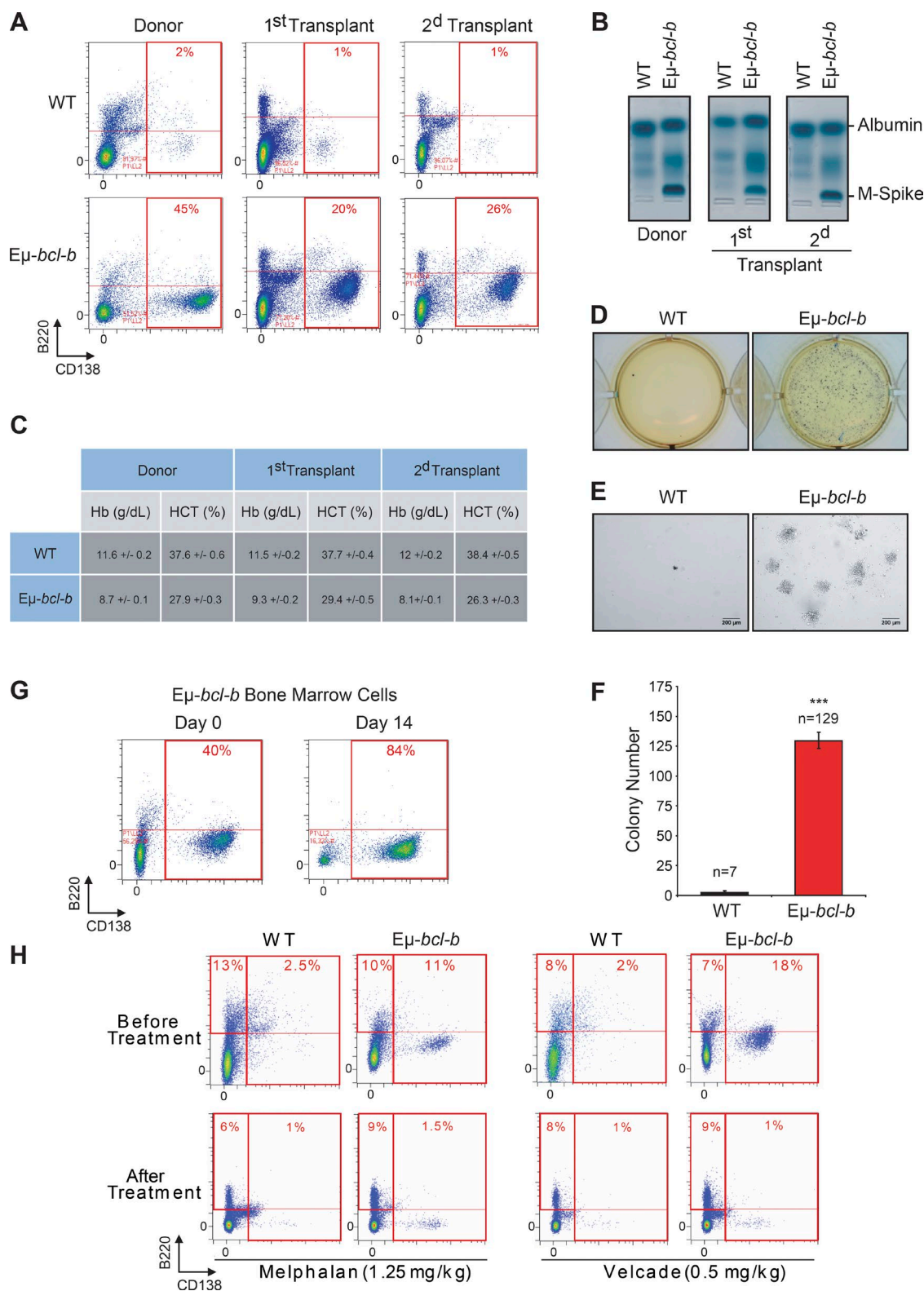


Figure 5. **The malignant PCs of $E\mu$ -*bcl-b* mice are serially transplantable and are sensitive to conventional MM therapies.** Mononuclear cells from the BM of either hemizygous 24-mo-old transgenic mice or control mice were isolated and injected i.v. into lethally irradiated syngeneic C57BL/6 mice. Two independent sets of recipient mice after a first and second serial transplant are represented. Transplanted mice were sacrificed at 3 mo. (A) The percentage of CD138⁺/B220⁺ PCs in control or $E\mu$ -*bcl-b* transplanted mice was determined by flow cytometry. (B) The presence of M-spike in the sera of

tion, B cells first exhibited increased expression of B220 (low to high) and next differentiated into B220⁺/CD138⁺ B cells (Fig. S1). Plasmacyte differentiation was assessed by following the emergence of B220⁺/CD138⁺ B cells in control and E μ -*bcl-b* mice. LPS significantly increased the proportion of B220⁺ B cells in transgenic mice (Fig. 6 B). Quantification of CD138⁺ cells revealed the increased differentiation potential of B cells isolated from E μ -*bcl-b* mice (Fig. 6 C). Collectively, these data show that Bcl-B favors plasmacyte differentiation. Expressions of Xbp-1 and PRDM1 were also analyzed because these transcription factors are known to be essential for plasmacyte differentiation. Xbp-1 has also been reported to drive MM in a transgenic mouse model (Carrasco et al., 2007). Xbp-1 and PRDM1 protein levels increased gradually during LPS-induced plasmacyte differentiation and correlated with plasmacyte differentiation in E μ -*bcl-b* mice (Fig. 6 D). CFSE staining experiments in splenocytes isolated from LPS-treated wild-type or E μ -*bcl-b* mice showed that differentiation of B cells (B220⁺/CD138⁻) into immature plasmacytes (B220⁺/CD138⁺) was more efficient in transgenic mice after 72 h. According to the release of CFSE, the inactive B220^{low}/CD138⁻ B cell population and B220^{low}/CD138⁺ mature plasmacytes from transgenic mice exhibited a strong increase in proliferative potential (Fig. 6 E). The proliferative potentials of active B220^{high}/CD138⁻ B cells and immature B220^{high}/CD138⁺ plasmacytes were slightly increased in the E μ -*bcl-b* mice. Finally, we performed experiments to determine whether the ability of Bcl-B to inhibit B cell death was responsible for increased differentiation, proliferation, and survival. In the absence of LPS, we detected a strong increase in plasmacyte cell death that was significantly lowered in E μ -*bcl-b*, whereas LPS induced a significant decrease in plasmacyte cell death in wild-type mice (Fig. 6 F). In addition, we observed marginal propidium iodide staining of plasmacytes from E μ -*bcl-b* mice, confirming the key role of Bcl-B in the protection against cell death. Identical results were observed for B cells (Fig. 6 F). No protection against cell death was detected in splenic T cells from wild type and E μ -*bcl-b* that did not express Bcl-B (Fig. 6 F). Globally, our data establish a specific role for Bcl-B in the differentiation and proliferation of plasmacytes through inhibition of cell death.

DISCUSSION

Molecular analysis of both mouse and human MM has underscored the important role of the antiapoptotic members of

the Bcl-2 family in the pathogenesis of this disease. Among them, Bcl-2 and Mcl-1 expression levels have been reported to be increased in MM and to act as key factors in MM disease progression and chemoresistance (Tu et al., 1998; Spets et al., 2002; Gomez-Bougie et al., 2004; Wuillème-Toumi et al., 2005; Bodet et al., 2011; Morales et al., 2011). In the present study, we examined a large panel of MM cell lines to determine the expression of Bcl-2, Mcl-1, and Bcl-B (Fig. 1, D and E). Importantly, Bcl-B protein level was homogeneous in all of the MM cell lines tested. Moreover, we clearly demonstrated that Bcl-B protein is highly overexpressed in plasmacytes isolated from MM patients compared with those isolated from either healthy controls or MGUS patients. These results suggest that, in addition to Bcl-2 and Mcl-1, Bcl-B protein may likely be a new marker of MM.

Owing to the importance of Bcl-2 members in the MM disease, several animal transgenic models were generated in which these antiapoptotic proteins were expressed in the B cell compartment. Enforced expression of Bcl-2 and Mcl-1 in B cells and hematopoietic cells, respectively, resulted in B cell malignancies displaying immature phenotype rather than MM (McDonnell and Korsmeyer, 1991; Zhou et al., 2001). Because Bcl-X_L is one of the most potent prosurvival proteins (Beverly and Varmus, 2009) and because Bcl-X_L is involved in chemoresistance processes in MM (Tu et al., 1998), a 3'KE/*Bcl-X_L* mouse model was engineered. Enforced expression of Bcl-X_L in B cells at late stage resulted in nonmalignant PC foci in the BM and soft tissues without affecting the life span of transgenic mice (Linden et al., 2004). When deregulation of Bcl-X_L and of the *c-Myc* oncogene was combined in the B cell compartment (3'KE/*Bcl-X_L*/Ig-Myc), mice developed nonindolent PC tumors with short onset (135 d on average) and full penetrance (Cheung et al., 2004). These tumors produced monoclonal Ig (IgG and IgM) and infiltrated BM as well as spleen. Moreover, PCs obtained from tissues with plasmacytosis were not transplantable into nude mice, suggesting that these cells had not yet undergone malignant transformation. These results suggest that deregulation of Bcl-X_L either alone or in combination with *c-Myc* oncogene in the B cell compartment does not drive a complete MM-like disease.

Of the different transgenic mice models expressing an antiapoptotic Bcl-2 member alone or together with *c-MYC* in the B cell compartment, the E μ -*bcl-b* model described herein is the only one that recapitulates most of the main features of the human MM pathology: reduction of life span,

serially transplanted mice was determined by SPEP analysis. (C) Hemoglobin and hematocrit levels were measured on a Hemavet automated cell counter. The mean \pm SD of three independent experiments is shown. (D) BM nucleated cells were isolated from 3-mo-old E μ -*bcl-b* or WT secondary transplanted mice and were grown in semisolid methyl cellulose medium (5×10^3 cells/ml). Colonies were detected after 14 d of culture by adding 1 mg/ml MTT reagent. (E) Light microscopy images of colonies were also captured. Bars, 200 μ m. (F) Colonies were counted using the ImageJ quantification software. (G) BM cells from E μ -*bcl-b* mice were also maintained in culture in StemSpan SFEM medium supplemented with 1 ng/ml of recombinant mouse-IL-7, and the proportion of PCs was determined by flow cytometry. (H) BM cells from 24-mo-old control and hemizygous E μ -*bcl-b* mice were isolated, and the percentage of plasmacytes (CD138⁺) was determined by cytometry. Then, mice were treated with either VELCADE (0.5 mg/kg twice a week for 6 wk) or melphalan (1.25 mg/kg once a day for 5 wk). At the end of the experiment, mice were sacrificed and plasmacytosis was monitored by flow cytometry as described above. Where indicated, the cumulative data \pm SD from independent experiments are shown. ***, $P < 0.001$, using a two-tailed Student's *t* test for unpaired data.

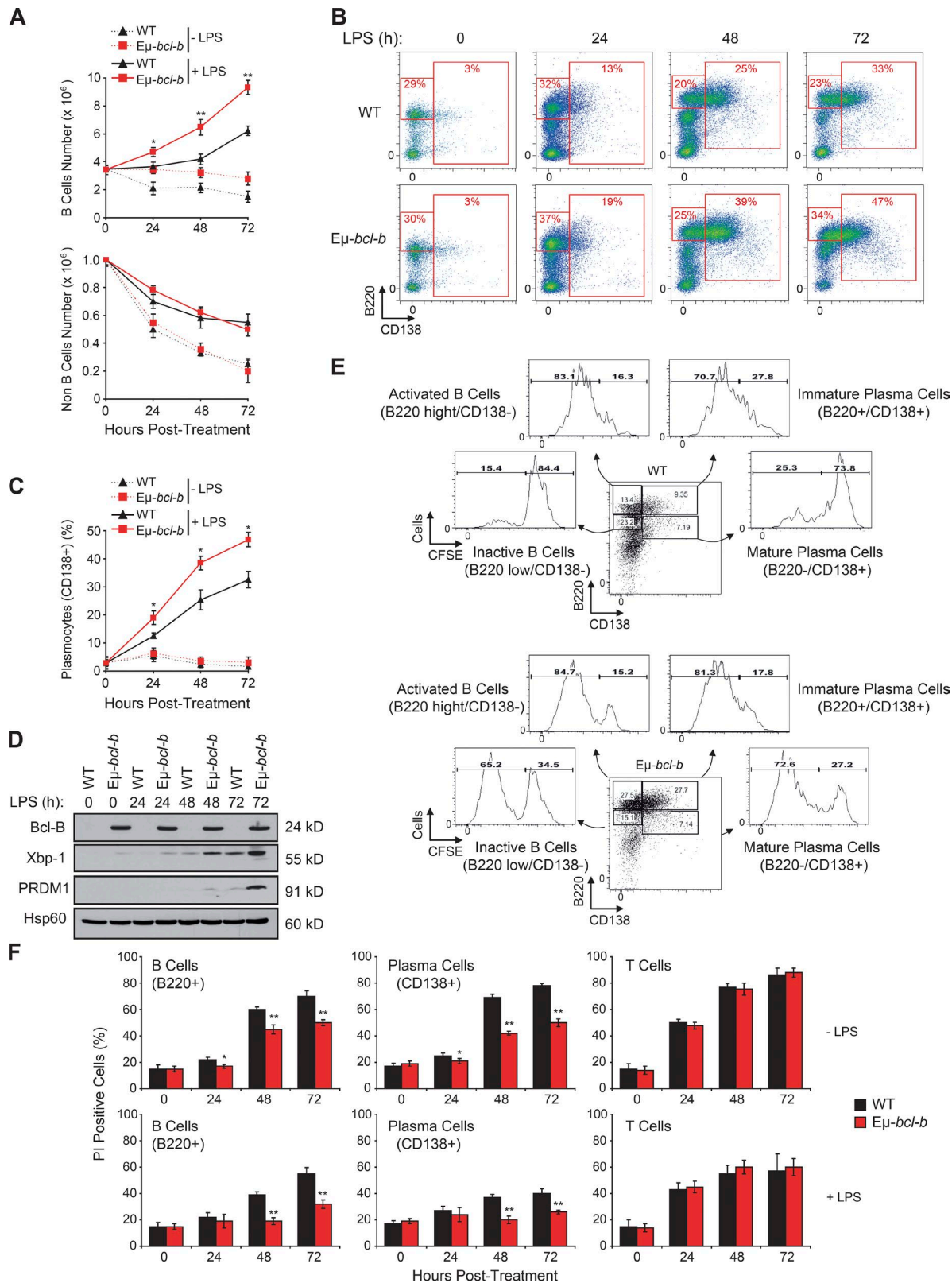


Figure 6. *Eμ-bcl-b* splenic cells show increased cell proliferation and differentiation. (A) Splenic B cells from hemizygous *Eμ-bcl-b* and WT mice were isolated and treated ex vivo for 1, 2, or 3 d with or without 8 μ g/ml LPS. The cells were then harvested, and the number of B and T cells was determined by flow cytometry using a B220 antibody. (B) Splenic cells from hemizygous *Eμ-bcl-b* or WT mice were treated as in A. The cells were then harvested,

high penetrance of phenotype, indolent PC expansion restricted to the BM, monoclonal gammaglobulinemia for the great majority of the homozygous mice (M-spike and unique IgG2b secretion), malignancy of the plasmocytes (transplantability into recipient mice), bone lytic lesions, renal immunoglobulin deposition, anemia, decreased albumin levels, and elevated expression of genes encoding proteins involved in MM pathogenesis.

Importantly, MM induction seems to be a unique feature of Bcl-B because the introduction of a prosurvival signal in the B cell compartment by other Bcl-2 members, even more robust ($E\mu$ -*bcl-2* or 3'KE/*bcl-x_L*) than the one induced by Bcl-B (Beverly and Varmus, 2009; Beverly et al., 2012), does not specifically lead to an MM-like disease in mice.

From the M-spike present in the sera of all the transgenic mice tested (Fig. 3, B and C), it is obviously impossible to extrapolate for a single VDJ rearrangement. However, (a) the ELISA tests performed on a great number of transgenic mice that specifically show the production of a unique monoclonal antibody (IgG2b), (b) the fact that $E\mu$ -*bcl-b* mice always exhibit >10% tumoral plasmocytes, and (c) the clonality data presented in Table S3 argue strongly that $E\mu$ -*bcl-b* mice do develop an MM phenotype. In addition, SHM, a hallmark of MM, was also confirmed in a few mice (Table S3). The percentage of mutations was significantly higher in transgenic mice, and although we used a random polymerase for the assessment of the VDJ rearrangement, previous results from our team have shown a mean error of <0.3% using this polymerase, which is drastically lower than the frequency of mutation found in $E\mu$ -*bcl-b* mice (unpublished data). These data convincingly show that $E\mu$ -*bcl-b* mice display an MM phenotype that replicates accurately the human disease. Another point of the present study is the specific expression of IgG2b by all $E\mu$ -*bcl-b* homozygous mice. Despite the fact that around 10–15% of all human MM secrete this specific isotype, we found no likely reason either in the literature or in questioning experts in the field that could explain such a selective IgG2b expression.

Of note, the *vk-Myc* mouse model of MM, in which the activation of *c-Myc* oncogene occurs sporadically throughout the physiological SHM process, shares many common features with our $E\mu$ -*bcl-b* mice. This model fulfills most of the biological and genetic criteria of an ideal mouse model of MM. Authors (Chesi et al., 2008) have argued that *c-myc*

activation could be the secondary event that further increases cell proliferation. One hypothesis could be that deregulation of Bcl-B in plasmocytes might represent an important primary prosurvival event necessary for the initiation of MM pathogenesis. This hypothesis is supported by the gene transcription profile that showed an increase of *c-myc* mRNA in plasmocytes isolated from $E\mu$ -*bcl-b* mice compared with control mice (Fig. 4). Table S4 summarizes the characteristics of the different MM-like mouse models previously generated.

Compared with other prosurvival Bcl-2 proteins, it was recently confirmed that Bcl-B has the narrowest capacity to bind proapoptotic proteins (Bax, Bik, and Bim), highlighting a more specialized role in the apoptosis signaling (Rautureau et al., 2012). The proapoptotic Bcl-2 protein Bim was reported to be essential for the maintenance of B cell homeostasis (Oliver et al., 2006; Huntington et al., 2009) through the elimination of autoreactive B cells (Enders et al., 2003; Fischer et al., 2007) and through its contribution to the differentiation of B cells into PCs (Gao et al., 2012). Moreover, expression of Bim and its association with the antiapoptotic Bcl-2 members was also described as an important factor for the survival of Myeloma cells (Gomez-Bougie et al., 2004; Romagnoli et al., 2009; Morales et al., 2011) and for the predicted response to chemotherapy agents. Thus, the specific and potent inhibition of Bim-induced cell death by Bcl-B could partially explain why $E\mu$ -*bcl-b* mice develop characteristic features of human MM.

In this context, a recent study suggested that the antiapoptotic potency of Bcl-2 proteins relies on their stability rather than their binding selectivity (Rooswinkel et al., 2014). Several studies are currently underway to better understand the mode of regulation of the Bcl-B protein in cells. Recent reports showed that ubiquitination and proteasomal turnover dictate the expression level of the Bcl-B protein and thereby its antiapoptotic activity (Beverly et al., 2012; van de Kooij et al., 2013; Rooswinkel et al., 2014). This work is in agreement with an alternative posttranslational stabilization mechanism as the main mode of Bcl-B regulation in MM. Using CHX, a protein synthesis inhibitor, we recently measured the stability of the Bcl-B protein in several non-MM and MM cell lines (unpublished data). We evaluated that the half-life of the Bcl-B protein in HeLa cells is ~3 h, which is consistent with previous studies describing Bcl-B as an unstable protein (Beverly et al., 2012; van de Kooij et al., 2013). In contrast, in MM

and the percentages of inactive B cells ($B220^{low}/CD138^{-}$), active B cells ($B220^{high}/CD138^{-}$), and immature/mature PCs ($CD138^{+}$) were determined by flow cytometry using B220 and CD138 antibodies. (C) The graph represents a quantification of the CD138-positive PCs after LPS treatment. (D) Splenic B cells from hemizygous $E\mu$ -*bcl-b* and WT mice were treated as in A. The cells were then collected, washed, and lysed, and total protein extracts were subjected to SDS-PAGE/immunoblot using Bcl-B, Xbp-1, PRDM1, and Hsp60 antibodies. (E) Splenic B cells from hemizygous $E\mu$ -*bcl-b* and WT mice were isolated and stained with CFSE dye. After 24 h, the cells were stimulated with 8 μ g/ml LPS for 72 h to induce plasmocyte differentiation. The proliferative potentials of the different living populations (inactive B cells [$B220^{low}/CD138^{-}$], active B cells [$B220^{high}/CD138^{-}$], immature PCs [$B220^{+}/CD138^{+}$], and mature PCs [$B220^{-}/CD138^{+}$]) were determined by flow cytometry. (F) Splenic B cells from hemizygous $E\mu$ -*bcl-b* and WT mice were treated as in A. Unstimulated cells (top) or LPS-stimulated cells (bottom) were harvested, washed, and labeled using B220 and CD138 antibodies as well as propidium iodide (PI). The percentage of dead cells (PI positive) was measured by flow cytometry. Where indicated, the cumulative data \pm SD from three independent experiments are shown. **, $P < 0.01$; *, $P < 0.05$, using a two-tailed Student's *t* test for unpaired data.

cells, Bcl-B remains stable at 24 h, suggesting an abnormal stability of this protein in this pathological context. Thus, even if the abnormal stability of the Bcl-B protein in MM appears to be a cause of its overexpression, the exact mechanism remains to be clarified and will be the object of future studies.

Importantly, E μ -*bcl-b* mice exhibit elevated expression of genes encoding proteins involved in MM pathogenesis that may contribute to the MM phenotype. A dedicated transcriptional profile of E μ -*bcl-b* BM plasmacytes showed increased expression of proto-oncogenes (*ccnd2*, *c-myc*, *c-maf*, and *c-jun*) that are well reported to be deregulated in the human MM (Claudio et al., 2002; Davies et al., 2003), therefore confirming the tumorigenic nature of the PCs we observed in our MM mouse model. The transcription factor *xbp-1*, required for PC proliferation and differentiation, was also induced in transgenic mice (Carrasco et al., 2007). This positive modulation is in agreement with the exacerbated proliferation and differentiation potential we observed in the B lymphocytes and plasmacytes of our mouse model. We also observed in E μ -*bcl-b* mice an increased expression of cytokines required for the survival and proliferation of PCs (*il-6*, *il-7*, and *igf-1*) and factors involved in osteoclastogenesis, including *trap*, *rank*, and *rank-l*. Among them, IL-6 and IGF-1 were obviously reported to be crucial for the survival and the proliferation of myeloma cells (Gaillard et al., 1997; Sprynski et al., 2009). IL-6 and IL-7, which are excessively secreted by tumor PCs, were also described to induce *rank-l* expression via stromal cells and thereby promote osteoclastogenesis (Giuliani et al., 2002). This perturbation of bone homeostasis is associated with the development of osteolytic lesions and the loss of bone volume observed in MM patients (Hjertner et al., 2006). Thus, increased mRNA expression of *il-6*, *il-7*, *rank*, and *rank-l* in our MM model is compatible with the bone lytic lesions we underlined. In summation, this gene network, which includes proto-oncogenes, master transcription factors involved in plasmacyte differentiation, cytokines implicated in plasmacyte survival, and proliferation and bone resorption factors, coincides strongly with the MM phenotype of our E μ -*bcl-b* mice.

In conclusion, we report here that the E μ -*bcl-b* transgenic mouse is a relevant model of human MM that accurately recapitulates the pathogenesis of this hematopoietic malignancy. Our data also underscore an as of yet unidentified role for Bcl-B in B cell proliferation and plasmacyte differentiation through its ability to impair B cell death and drive MM progression. High levels of Bcl-B protein were also observed in patients with MM but not in healthy controls or patients with MGUS. As this model recapitulates accurately the human disease and is readily transplantable in secondary recipients, it represents a pertinent tool to validate new potential therapies for MM patients.

MATERIALS AND METHODS

E μ -*bcl-b* transgenic mice

To drive the expression of the Bcl-B protein in B cells, we used the pBlueScript II vector containing a mouse variable chain

enhancer, a promoter (E μ), a fragment of the rabbit β -globin gene, and a polyadenylation signal sequence. The Myc-tagged *bcl-b* cDNA was amplified by PCR from the corresponding pcDNA3 plasmid (Luciano et al., 2007) using the following primers: forward 5'-ATACTCGAGATGGAACAGAACTCATCTCT-3' and reverse 5'-ATACTCGAGTCATAATAATCGTGTCCAGAG-3'. Each primer contains an Xho1 restriction site. The pBlueScript-Myc-*bcl-b* vector was obtained by subcloning the Xho1-digested Myc-*bcl-b* PCR fragment into the Xho1-digested pBlueScript vector. After sequencing, the vector sequence was excised by SacI-KpnI digestion, and the resulting linearized and purified sequence was micro-injected into pronuclei obtained from B6D2 mice (Service d'Experimentation Animale et de Transg n se [SEAT], CNRS, Villejuif, Paris, France). Transgenic founders were crossed with C57BL/6N mice to generate lines. F1 transgenic progeny were crossed with C57BL/6N mice to maintain the lines, and the mice were kept in specific pathogen-free conditions at the C3M facility for all subsequent analyses. The described phenotype of the E μ -*bcl-b* mice was maintained through at least 10 generations. Screening of the transgenic mice was performed by PCR analysis using a set of *bcl-b*-specific primers (5'-GCC AACCTTTGTTCATGGC-3' and 5'-GTGGTGACGCTC GTGACC-3'), and the expression of the Bcl-B protein was confirmed by Western blot analysis of various tissues using an anti-Bcl-B antibody (compare Table S1).

For the survival experiments, the mice were aged until they showed evident signs of tumors and/or discomfort and subsequently sacrificed. Sibling control mice were sacrificed at the same time or allowed to age further. Necropsy was performed to assess the presence of phenotypic abnormalities. Statistical analysis was performed using Prism software (Graph-Pad Software). Survival curves were generated using the Kaplan-Meier method. All animal studies and experiments were performed with the approval of the Comit  Institutionnel d'Ethique Pour l'Animal de Laboratoire (CIEPAL) and were in agreement with all regulatory standards. After the eradication of all our mice, the E μ -*bcl-b* strain has been now rederived (JANVIER Labs; project number 15.355), so that this model will be fully available for the scientific community in 2017.

Cell lines

The human MM cell lines U266, MM1.S, NCI-H929, RPMI8226, ARH-77, AF-10, and OPM2 were purchased from ATCC. The LP-1 cell line was obtained from DSMZ. The JIM3, XG-1, XG-2, XG-5, XG-7, MDN, JIM-3, Nan-1, Nan-3, Nan-8, BCN, and SBN cell lines were provided by M. Amiot (INSERM U892, Nantes, France). All cells were cultured in RPMI-1640 medium containing 10% fetal bovine serum, 50 U/ml penicillin, 50 mg/ml streptomycin, and 1 mM sodium pyruvate (Gibco).

Western blot analysis

Whole cell extracts from BM, splenocytes, snap-frozen tissues, and MM cell lines were lysed at 4 C in lysis buffer (50 mM

Hepes, pH 7.4, 150 mM NaCl, 20 mM EDTA, 100 μ M NaF, 10 μ M Na₃VO₄, 1 mM PMSE, 10 mg/ml leupeptin, 10 mg/ml aprotinin, and 1% Triton X-100). The lysates were centrifuged at 16,000 *g* for 15 min at 4°C, and the supernatants were supplemented with SDS sample buffer. A total of 30 μ g of proteins was separated on a 12% SDS–polyacrylamide gel and transferred onto PVDF membranes (GE Healthcare) in 20 mM Tris, 150 mM glycine, and 20% ethanol buffer. After blocking nonspecific binding sites in saturation buffer (50 mM Tris, pH 7.5, 50 mM NaCl, 0.15% Tween, and 5% BSA), the membranes were probed with primary antibodies (compare with Table S1) according to standard procedures. The membranes were then washed three times using TNA–1% NP-40 (50 mM Tris, pH 7.5, and 150 mM NaCl) and incubated further for 1 h with HRP-conjugated antibodies. Bound immunoglobulins were detected using ECL detection solution (GE Healthcare).

Flow cytometry

Single-cell suspensions from spleens, thymuses, and BM were collected, and red blood cells were lysed by ammonium chloride treatment (Sigma-Aldrich). 10⁶ cells were washed in PBS (0.5% BSA and 2 mM EDTA) and stained for 30 min on ice with a combination of the indicated antibodies (compare with Table S1). Then, the cells were washed twice and resuspended in PBS (0.5% BSA and 2 mM EDTA). Multicolor flow cytometric analysis was performed using a MACSQuant cytometer (Miltenyi Biotec) and analyzed with MACSQuant software.

Isolation of PCs from patients

CD138⁺ BM cells were isolated from patients using magnetic CD138 microbeads (Miltenyi Biotec) according to the manufacturer's instructions. In brief, patient samples were collected in tubes containing EDTA. Then, the cells were passed through a filter (100- μ m pore size) to remove bone fragments or cell clumps. The cells were then centrifuged at 445 *g* for 10 min at room temperature in a swinging bucket rotor with the brake off. The supernatant was aspirated, and the cells were incubated with 50 μ l of whole blood CD138 microbeads per 1 ml of anticoagulated BM for 15 min at 4°C. The cells were then washed and resuspended in autoMACS running buffer. The magnetic separation was performed using the Possel WB program on the autoMACS Pro Separator. The purity of the isolated PCs was assessed by flow cytometry using an anti-human CD138 antibody (compare with Table S1).

Treatment of *E μ -bcl-b* mice with VELCADE and melphalan

E μ -bcl-b mice with significant plasmacytosis (>15%) were selected for drug treatment (five mice per group). 0.5 mg/kg VELCADE was given twice a week for 6 wk. 1.25 mg/kg melphalan was given once a day (5 d per week) for 5 wk. Treatments with VELCADE and melphalan were administered intraperitoneally with insulin syringe. At the end of the experiment, mice were sacrificed, and the BM plasmacytosis was quantified by flow cytometry.

Isolation of PCs from mice

The isolation of mouse PCs was performed with a CD138⁺ PC isolation kit (Miltenyi Biotec) according to the manufacturer's instructions. In brief, cells were extracted from tibia and femora of either *E μ -bcl-b* or control mice, and the isolation of mouse PCs was performed in a two-step procedure. First, non-PCs were magnetically labeled with a cocktail of biotin-conjugated antibodies (CD49b and CD45R) and anti-biotin microbeads. Cells were then separated with autoMACS Separator (program Depl025). In the second step, PCs contained in the negative fraction were directly labeled with CD138 microbeads and isolated by positive selection (program Posseld2). The purity of the isolated PCs was assessed by flow cytometry using anti-mouse CD138 and B220 antibodies.

Ex vivo culture of splenocytes

8–10-wk-old WT or *E μ -bcl-b* mice were euthanized, and single-cell splenocyte suspensions were obtained by dissociation of the corresponding spleen. After red blood cell lysis with ammonium chloride (Sigma-Aldrich), the splenocytes were counted and plated at a density of 5×10^5 cells/ml in splenocyte medium (RPMI-1640 medium containing 10% fetal bovine serum, 50 U/ml penicillin, 50 mg/ml streptomycin, 1 mM sodium pyruvate, and 50 μ M 2-ME). Then, the splenocytes were incubated with 8 μ g/ml LPS serotype B4 (Sigma-Aldrich). The experiment was terminated after 1, 2, or 3 d.

In vitro proliferation assay

B220⁺ splenocytes were incubated with 5 μ M CellTrace CFSE (Invitrogen) for 15 min at 37°C according to the manufacturer's instructions. Then, the cells were washed and plated in the splenocyte medium described in the previous section. After 18 h, the cells were washed and plated in the same medium in the presence or absence of 8 μ g/ml LPS and grown for 1, 2, or 3 d. The cells were then harvested and washed, and B cells were phenotyped using anti-mouse B220 and anti-mouse CD138 antibodies (compare Table S1). In parallel, the proliferative potential (as measured by CFSE release) of the different living populations was determined by flow cytometry.

Colony formation assay

BM nucleated cells were isolated from the femora and tibia of *E μ -bcl-b* or WT recipient mice. After red blood cell lysis with ammonium chloride (Sigma-Aldrich), BM cells were grown in semisolid methyl cellulose medium (0.5×10^3 cells/ml; MethoCult M3630; STEMCELL Technologies). Colonies were visualized after 14 d of culture by adding 1 mg/ml 3-(4,5-dimethylthiazol-2-yl)-2,5-diphenyltetrazolium bromide (MTT) reagent and were counted using the ImageJ quantification software (National Institutes of Health).

Ex vivo culture of BM cells

BM nucleated cells were isolated from the femora and tibia of *E μ -bcl-b* or WT recipient mice. After red blood cell lysis with ammonium chloride (Sigma-Aldrich), the BM cells

were counted and plated at a density of 5×10^5 cells/ml in StemSpan SFEM medium (STEMCELL Technologies) supplemented with 1 ng/ml recombinant mouse-IL-7 (Miltenyi Biotec). Cells were maintained in culture for 14 d.

Quantitative reverse transcription PCR

Total RNA was prepared from the BM cells of 18-mo-old transgenic mice or their control littermates using TRIzol reagent according to the manufacturer's instructions (Invitrogen). Total RNA (1 μ g) was reverse transcribed into cDNA using Superscript II reverse transcription (Invitrogen). Quantitative PCR was performed using 100 ng cDNA and Power SYBR Green PCR Master Mix (Applied Biosystems). Each sample was run in triplicate in a Step One Plus Real-Time PCR System (Applied Biosystems). The primers used are listed in Table S2. The expression levels were normalized to that of the *ubiquitin* and β -*actin* housekeeping genes. The results were analyzed using the comparative $2^{-\Delta\Delta C_t}$ method, with WT expression normalized to 1.

IgVH rearrangement and SHM analysis

The rearranged immunoglobulin variable heavy-chain region (IgVH) genes were amplified from DNA isolated from purified tumor and normal PCs by PCR. Forward primers that anneal to framework region III of the most abundantly used Igh-VJ558 and Igh-V7183 were used in separate reactions (covering >80% of the rearrangements) along with a reverse primer downstream of JH4. Immunoglobulin kappa light (IgK) chain rearrangements were PCR amplified using VK consensus primers and a reverse primer downstream of JK5. The PCR conditions were 40 cycles of 95°C for 30 s, 60°C for 45 s, and 72°C for 90 s. PCR products indicative of clonal rearrangements were gel purified using the Wizard Gel and PCR clean-up kit (Promega) and were sequenced directly using the same primers as in the PCR reaction and then further cloned using the PGEm-T Easy kit (Promega). 5–10 clones were sequenced for each PCR fragment to evaluate the clonal dominance of a given rearrangement. To determine IgV rearrangement and calculate the mutation frequency, sequences were aligned to the NCBI databases (IgBlast) and confirmed using the international ImMunoGeneTics information system (IMGT) database. PCR for IgH and IgK was repeated two or three times for each sample to confirm the presence of dominant PCR fragments in tumors and of polyclonal patterns in WT PCs. As a control, DNA extracted from mouse normal PCs were analyzed in parallel to calculate the SHM rate.

X-ray analysis, TRAP staining, histopathology, and immunohistochemistry

Bone x-ray radiography was performed on aged WT and $E\mu$ -*bcl-b* freshly isolated non-decalcified femurs using the Faxitron x-ray Edimex System and AGFA HDR 37F9H films.

Kidneys were fixed in 4% paraformaldehyde for 2 h at room temperature and then overnight at 4°C. Fixed tissues

were embedded into optimal cutting temperature media (OCT) and frozen in liquid nitrogen. OCT blocks containing the tissues were stored at -80°C until they were sectioned. Using a Leica cryostat CM350 (C3M histology facility, Nice), 10- to 15- μm sections were collected. The tissue sections were incubated for 1 h with 1% Congo red solution, rinsed in water, and cleared in alkaline alcohol until a clear background was obtained. Nuclei were then labeled with Harris hematoxylin for 30 s and rinsed in running water for 5–10 min. Sections were mounted in glycerol-based solution, and brightfield and polarized images were acquired on a Leica DM5500B microscope equipped with a polarizer and a color camera (C3M light microscopy facility, Nice).

Femurs were fixed and decalcified in Bouin's fixative solution (Labonord). After decalcification, the bones were dehydrated through a graded alcohol series and xylene and subsequently embedded in paraffin. 5- μm sections were cut and stained with hematoxylin and eosin (H&E). Immunohistochemistry was performed using a BenchMark XT Automated IHC Slide Staining System (Ventana; Roche) according to standard procedures. Dewaxed tissue sections were stained using an anti-mouse CD138 rat polyclonal antibody followed sequentially by mouse anti-rat biotinylated and streptavidin HRP antibodies (compare with Table S1).

TRAP staining

Femora were fixed in 4% paraformaldehyde for 24 h at 4°C, decalcified in 10% EDTA for 10 d at 4°C, and incubated overnight in a 30% sucrose solution, and 7- μm sections were obtained with a cryotome (Shandon; Thermo Fisher Scientific). Bone sections were stained for TRAP activity using a leukocyte acid phosphatase kit (Sigma-Aldrich) and hematoxylin, and staining was visualized by light microscopy (Palm Micro Beam; ZEISS). TRAP staining was analyzed in the trabecular zone of the femora as described (Mansour et al., 2011): images were analyzed using ImageJ software (W. Rasband, National Institutes of Health Image System) to define the areas corresponding to TRAP staining. These areas were normalized to the bone areas.

Hemoglobin, paraprotein (SPEP), and immunoglobulin measurement

Peripheral blood from WT and $E\mu$ -*bcl-b* mice was collected into tubes containing EDTA (Greiner Bio-One). Hemoglobin levels were measured on a Drew Hemavet 950FS and compared using the two-tailed Student's *t* test for unpaired data. For paraprotein measurement, the mice were bled by tail grazing. Then, the blood was collected, and the sera were harvested after blood coagulation and centrifugation for 10 min at 1,000 *g*. The sera were diluted 1:2 in barbital buffer (60 mM Tris, 10 mM barbital, 50 mM Na-diethyl-barbituric acid, 0.5 μM thimerosal). Then, the sera were loaded onto gels and separated by electrophoresis (1% agarose [Euromedex] polymerized in barbital buffer). The gels were stained with

amido black and destained with acetic acid. For immunoglobulin measurement, the sera were diluted 1:50, and the total Ig concentrations were determined using an Ig subtype-specific ELISA quantification kit (Thermo Fisher Scientific). It has been reported that some anti-IgG2a could cross-react with IgG2c. Nevertheless, there was no difference between IgG2a expression between WT and transgenic mice, ruling out the possibility of an increased expression of IgG2c. This means that IgG2b is the only monoclonal antibody overexpressed in the E μ -*bcl-b* mice.

BM transplantation

BM nucleated cells were isolated from E μ -*bcl-b* or WT femora and tibia donor mice. Then, 20 million cells were resuspended in 100 μ l PBS and transplanted by i.v. injection into the tails of 10-wk-old WT C57BL/6 recipient mice irradiated with 7Gy.

Statistical analysis

The results are expressed as the mean \pm SD. The data were compared by one-way ANOVA and Student's *t* tests, and the Bonferroni correction was applied using GraphPad Prism software. Statistical significance was established at ***, *P* < 0.0001; **, *P* < 0.01; *, *P* < 0.05. Survival rates were compared with the Kaplan-Meier method using Prism software.

Study approval

BM samples from healthy, MGUS, or myeloma patients were obtained from the Internal Medicine or Hematology Departments of the Centre Hospitalier Universitaire de Nice after informed consent was obtained (clinical trial NCT01270009). Mouse experiments were approved by the Institutional Animal Care and Use committee of the University of Nice Sophia-Antipolis (Nice, France).

Online supplemental material

Fig. S1 shows a schematic representation of B cell activation and differentiation after LPS stimulation. Table S1 shows a list of antibodies used for flow cytometry, Western blot, and immunochemistry. Table S2 shows a list of primers used for quantitative PCR. Table S3 shows IgH and IgK gene rearrangement and somatic mutations in mouse tumors. Table S4 shows a comparison of the biological and clinical features of available MM mouse models. Online supplemental material is available at <http://www.jem.org/cgi/content/full/jem.20150983/DC1>.

ACKNOWLEDGMENTS

We are grateful to our clinician colleagues from the Centre Hospitalier Universitaire de Nice. We also sincerely thank all patients enrolled in this study. We greatly acknowledge the C3M imaging core facility (Microscopy and Imaging Platform Côte d'Azur, Mica) and the C3M animal facility.

This work was supported by the Ligue Nationale Contre le Cancer (Equipe Labelisée grant R08001AA), the Fondation de France (grant R08080AA), and an ARC Foundation program (grant PGA120140200777) and an ARC project (2015–2016). This work was also funded by the French government (French National Research Agency,

ANR) through the "Investments for the future" LABEX SIGNALIFE: program reference #ANR-11-LABX-0028-01.

The authors declare no competing financial interests.

Submitted: 12 June 2015

Accepted: 6 June 2016

REFERENCES

- Adams, J.M., and S. Cory. 1998. The Bcl-2 protein family: arbiters of cell survival. *Science*. 281:1322–1326. <http://dx.doi.org/10.1126/science.281.5381.1322>
- Beverly, L.J., and H.E. Varmus. 2009. MYC-induced myeloid leukemogenesis is accelerated by all six members of the antiapoptotic BCL family. *Oncogene*. 28:1274–1279. <http://dx.doi.org/10.1038/onc.2008.466>
- Beverly, L.J., W.W. Lockwood, P.P. Shah, H. Erdjument-Bromage, and H. Varmus. 2012. Ubiquitination, localization, and stability of an anti-apoptotic BCL2-like protein, BCL2L10/BCLb, are regulated by Ubiquilin1. *Proc. Natl. Acad. Sci. USA*. 109:E119–E126. <http://dx.doi.org/10.1073/pnas.1119167109>
- Bodet, L., P. Gomez-Bougie, C. Touzeau, C. Dousset, G. Descamps, S. Maïga, H. Avet-Loiseau, R. Bataille, P. Moreau, S. Le Gouill, et al. 2011. ABT-737 is highly effective against molecular subgroups of multiple myeloma. *Blood*. 118:3901–3910. <http://dx.doi.org/10.1182/blood-2010-11-317438>
- Borson, N.D., M.Q. Lacy, and P.J. Wettstein. 2002. Altered mRNA expression of Pax5 and Blimp-1 in B cells in multiple myeloma. *Blood*. 100:4629–4639. <http://dx.doi.org/10.1182/blood.V100.13.4629>
- Boylan, K.L., M.A. Gosse, S.E. Staggs, S. Janz, S. Grindle, G.S. Kansas, and B.G. Van Ness. 2007. A transgenic mouse model of plasma cell malignancy shows phenotypic, cytogenetic, and gene expression heterogeneity similar to human multiple myeloma. *Cancer Res*. 67:4069–4078. <http://dx.doi.org/10.1158/0008-5472.CAN-06-3699>
- Carrasco, D.R., G. Tonon, Y. Huang, Y. Zhang, R. Sinha, B. Feng, J.P. Stewart, F. Zhan, D. Khatry, M. Protopopova, et al. 2006. High-resolution genomic profiles define distinct clinico-pathogenetic subgroups of multiple myeloma patients. *Cancer Cell*. 9:313–325. <http://dx.doi.org/10.1016/j.ccr.2006.03.019>
- Carrasco, D.R., K. Sukhdeo, M. Protopopova, R. Sinha, M. Enos, D.E. Carrasco, M. Zheng, M. Mani, J. Henderson, G.S. Pinkus, et al. 2007. The differentiation and stress response factor XBP-1 drives multiple myeloma pathogenesis. *Cancer Cell*. 11:349–360. <http://dx.doi.org/10.1016/j.ccr.2007.02.015>
- Chesi, M., D.F. Robbani, M. Sebag, W.J. Chng, M. Affer, R. Tiedemann, R. Valdez, S.E. Palmer, S.S. Haas, A.K. Stewart, et al. 2008. AID-dependent activation of a MYC transgene induces multiple myeloma in a conditional mouse model of post-germinal center malignancies. *Cancer Cell*. 13:167–180. <http://dx.doi.org/10.1016/j.ccr.2008.01.007>
- Cheung, W.C., J.S. Kim, M. Linden, L. Peng, B. Van Ness, R.D. Polakiewicz, and S. Janz. 2004. Novel targeted deregulation of c-Myc cooperates with Bcl-X_L to cause plasma cell neoplasms in mice. *J. Clin. Invest*. 113:1763–1773. <http://dx.doi.org/10.1172/JCI200420369>
- Claudio, J.O., E. Masih-Khan, H. Tang, J. Gonçalves, M. Voralia, Z.H. Li, V. Nadeem, E. Cukerman, O. Francisco-Pabalan, C.C. Liew, et al. 2002. A molecular compendium of genes expressed in multiple myeloma. *Blood*. 100:2175–2186. <http://dx.doi.org/10.1182/blood-2002-01-0008>
- Cluzeau, T., G. Robert, N. Mounier, J.M. Karsenti, M. Dufies, A. Puissant, A. Jacquel, A. Renneville, C. Preudhomme, J.P. Cassuto, et al. 2012. BCL2L10 is a predictive factor for resistance to azacitidine in MDS and AML patients. *Oncotarget*. 3:490–501. <http://dx.doi.org/10.18632/oncotarget.481>
- Davies, F.E., A.M. Dring, C. Li, A.C. Rawstron, M.A. Shammas, S.M. O'Connor, J.A. Fenton, T. Hideshima, D. Chauhan, I.T. Tai, et al. 2003.

- Insights into the multistep transformation of MGUS to myeloma using microarray expression analysis. *Blood*. 102:4504–4511. <http://dx.doi.org/10.1182/blood-2003-01-0016>
- De Vos, J., C. Bagnis, L. Bonnafox, G. Requirand, M. Jourdan, M.C. Imbert, E. Jourdan, J.F. Rossi, P. Mannoni, and B. Klein. 2003. Comparison of murine leukemia virus, human immunodeficiency virus, and adeno-associated virus vectors for gene transfer in multiple myeloma: lentiviral vectors demonstrate a striking capacity to transduce low-proliferating primary tumor cells. *Hum. Gene Ther.* 14:1727–1739. <http://dx.doi.org/10.1089/104303403322611746>
- Enders, A., P. Bouillet, H. Puthalakath, Y. Xu, D.M. Tarlinton, and A. Strasser. 2003. Loss of the pro-apoptotic BH3-only Bcl-2 family member Bim inhibits BCR stimulation-induced apoptosis and deletion of autoreactive B cells. *J. Exp. Med.* 198:1119–1126. <http://dx.doi.org/10.1084/jem.20030411>
- Fischer, S.F., P. Bouillet, K. O'Donnell, A. Light, D.M. Tarlinton, and A. Strasser. 2007. Proapoptotic BH3-only protein Bim is essential for developmentally programmed death of germinal center-derived memory B cells and antibody-forming cells. *Blood*. 110:3978–3984. <http://dx.doi.org/10.1182/blood-2007-05-091306>
- Gaillard, J.P., J. Liautard, B. Klein, and J. Brochier. 1997. Major role of the soluble interleukin-6/interleukin-6 receptor complex for the proliferation of interleukin-6-dependent human myeloma cell lines. *Eur. J. Immunol.* 27:3332–3340. <http://dx.doi.org/10.1002/eji.1830271232>
- Gao, Y., H. Kazama, and S. Yonehara. 2012. Bim regulates B-cell receptor-mediated apoptosis in the presence of CD40 signaling in CD40-pre-activated splenic B cells differentiating into plasma cells. *Int. Immunol.* 24:283–292. <http://dx.doi.org/10.1093/intimm/dxr127>
- Giuliani, N., S. Colla, R. Sala, M. Moroni, M. Lazzaretti, S. La Monica, S. Bonomini, M. Hojden, G. Sammarelli, S. Barillè, et al. 2002. Human myeloma cells stimulate the receptor activator of nuclear factor-kappa B ligand (RANKL) in T lymphocytes: a potential role in multiple myeloma bone disease. *Blood*. 100:4615–4621. <http://dx.doi.org/10.1182/blood-2002-04-1121>
- Gomez-Bougie, P., R. Bataille, and M. Amiot. 2004. The imbalance between Bim and Mcl-1 expression controls the survival of human myeloma cells. *Eur. J. Immunol.* 34:3156–3164. <http://dx.doi.org/10.1002/eji.200424981>
- Hjertner, Ø., T. Standal, M. Børset, A. Sundan, and A. Waage. 2006. Bone disease in multiple myeloma. *Med. Oncol.* 23:431–441. <http://dx.doi.org/10.1385/MO:23:4:431>
- Huntington, N.D., V. Labi, A. Cumano, P. Vieira, A. Strasser, A. Villunger, J.P. Di Santo, and N.L. Alves. 2009. Loss of the pro-apoptotic BH3-only Bcl-2 family member Bim sustains B lymphopoiesis in the absence of IL-7. *Int. Immunol.* 21:715–725. <http://dx.doi.org/10.1093/intimm/dxp043>
- Iida, S., P.H. Rao, M. Butler, P. Corradini, M. Boccadoro, B. Klein, R.S. Chaganti, and R. Dalla-Favera. 1997. Deregulation of MUM1/IRF4 by chromosomal translocation in multiple myeloma. *Nat. Genet.* 17:226–230. <http://dx.doi.org/10.1038/ng1097-226>
- Inohara, N., T.S. Gourley, R. Carrio, M. Muñoz, J. Merino, I. Garcia, T. Koseki, Y. Hu, S. Chen, and G. Núñez. 1998. Diva, a Bcl-2 homologue that binds directly to Apaf-1 and induces BH3-independent cell death. *J. Biol. Chem.* 273:32479–32486. <http://dx.doi.org/10.1074/jbc.273.49.32479>
- Ke, N., A. Godzik, and J.C. Reed. 2001. Bcl-B, a novel Bcl-2 family member that differentially binds and regulates Bax and Bak. *J. Biol. Chem.* 276:12481–12484. <http://dx.doi.org/10.1074/jbc.C000871200>
- Klein, B., K. Tarte, M. Jourdan, K. Mathouk, J. Moreaux, E. Jourdan, E. Legouffe, J. De Vos, and J.F. Rossi. 2003. Survival and proliferation factors of normal and malignant plasma cells. *Int. J. Hematol.* 78:106–113. <http://dx.doi.org/10.1007/BF02983377>
- Krajewska, M., S. Kitada, J.N. Winter, D. Variakojis, A. Lichtenstein, D. Zhai, M. Cuddy, X. Huang, F. Luciano, C.H. Baker, et al. 2008. Bcl-B expression in human epithelial and nonepithelial malignancies. *Clin. Cancer Res.* 14:3011–3021. <http://dx.doi.org/10.1158/1078-0432.CCR-07-1955>
- Linden, M., N. Kirchhof, C. Carlson, and B. Van Ness. 2004. Targeted overexpression of Bcl-XL in B-lymphoid cells results in lymphoproliferative disease and plasma cell malignancies. *Blood*. 103:2779–2786. <http://dx.doi.org/10.1182/blood-2003-10-3399>
- Luciano, F., M. Krajewska, P. Ortiz-Rubio, S. Krajewski, D. Zhai, B. Faustin, J.M. Bruey, B. Bailly-Maitre, A. Lichtenstein, S.K. Kolluri, et al. 2007. Nur77 converts phenotype of Bcl-B, an antiapoptotic protein expressed in plasma cells and myeloma. *Blood*. 109:3849–3855. <http://dx.doi.org/10.1182/blood-2006-11-056879>
- Ludwig, H., M. Beksac, J. Bladé, M. Boccadoro, J. Cavenagh, M. Cavo, M. Dimopoulos, J. Drach, H. Einsele, T. Facon, et al. 2010. Current multiple myeloma treatment strategies with novel agents: a European perspective. *Oncologist*. 15:6–25. <http://dx.doi.org/10.1634/theoncologist.2009-0203>
- Mansour, A., A. Anginot, S.J. Mancini, C. Schiff, G.F. Carle, A. Wakkach, and C. Blin-Wakkach. 2011. Osteoclast activity modulates B-cell development in the bone marrow. *Cell Res.* 21:1102–1115. <http://dx.doi.org/10.1038/cr.2011.21>
- McDonnell, T.J., and S.J. Korsmeyer. 1991. Progression from lymphoid hyperplasia to high-grade malignant lymphoma in mice transgenic for the t(14; 18). *Nature*. 349:254–256. <http://dx.doi.org/10.1038/349254a0>
- Morales, A.A., M. Kurtoglu, S.M. Matulis, J. Liu, D. Siefker, D.M. Gutman, J.L. Kaufman, K.P. Lee, S. Lonial, and L.H. Boise. 2011. Distribution of Bim determines Mcl-1 dependence or codependence with Bcl-xL/Bcl-2 in Mcl-1-expressing myeloma cells. *Blood*. 118:1329–1339. <http://dx.doi.org/10.1182/blood-2011-01-327197>
- Morito, N., K. Yoh, A. Maeda, T. Nakano, A. Fujita, M. Kusakabe, M. Hamada, T. Kudo, K. Yamagata, and S. Takahashi. 2011. A novel transgenic mouse model of the human multiple myeloma chromosomal translocation t(14;16)(q32;q23). *Cancer Res.* 71:339–348. <http://dx.doi.org/10.1158/0008-5472.CAN-10-1057>
- Ohguchi, H., T. Hideshima, M.K. Bhasin, G.T. Gorgun, L. Santo, M. Cea, M.K. Samur, N. Mimura, R. Suzuki, Y.T. Tai, et al. 2016. The KDM3A-KLF2-IRF4 axis maintains myeloma cell survival. *Nat. Commun.* 7:10258. <http://dx.doi.org/10.1038/ncomms10258>
- Oliver, P.M., T. Vass, J. Kappler, and P. Marrack. 2006. Loss of the proapoptotic protein, Bim, breaks B cell anergy. *J. Exp. Med.* 203:731–741. <http://dx.doi.org/10.1084/jem.20051407>
- Palumbo, A., and K. Anderson. 2011. Multiple myeloma. *N. Engl. J. Med.* 364:1046–1060. <http://dx.doi.org/10.1056/NEJMra1011442>
- Park, S.S., J.S. Kim, L. Tessarollo, J.D. Owens, L. Peng, S.S. Han, S. Tae Chung, T.A. Torrey, W.C. Cheung, R.D. Polakiewicz, et al. 2005. Insertion of c-Myc into Igh induces B-cell and plasma-cell neoplasms in mice. *Cancer Res.* 65:1306–1315. <http://dx.doi.org/10.1158/0008-5472.CAN-04-0268>
- Rautureau, G.J., M. Yabal, H. Yang, D.C. Huang, M. Kvensakul, and M.G. Hinds. 2012. The restricted binding repertoire of Bcl-B leaves Bim as the universal BH3-only prosurvival Bcl-2 protein antagonist. *Cell Death Dis.* 3:e443. <http://dx.doi.org/10.1038/cddis.2012.178>
- Romagnoli, M., C. Séveno, S. Wuillème-Toumi, M. Amiot, R. Bataille, S. Minvielle, and S. Barillè-Nion. 2009. The imbalance between Survivin and Bim mediates tumour growth and correlates with poor survival in patients with multiple myeloma. *Br. J. Haematol.* 145:180–189. <http://dx.doi.org/10.1111/j.1365-2141.2009.07608.x>
- Rooswinkel, R.W., B. van de Kooij, E. de Vries, M. Paauwe, R. Braster, M. Verheij, and J. Borst. 2014. Antiapoptotic potency of Bcl-2 proteins primarily relies on their stability, not binding selectivity. *Blood*. 123:2806–2815. <http://dx.doi.org/10.1182/blood-2013-08-519470>
- Shaffer, A.L., N.C. Emre, L. Lamy, V.N. Ngo, G. Wright, W. Xiao, J. Powell, S. Dave, X. Yu, H. Zhao, et al. 2008. IRF4 addiction in multiple myeloma. *Nature*. 454:226–231. <http://dx.doi.org/10.1038/nature07064>

- Spets, H., T. Strömberg, P. Georgii-Hemming, J. Siljason, K. Nilsson, and H. Jernberg-Wiklund. 2002. Expression of the bcl-2 family of pro- and anti-apoptotic genes in multiple myeloma and normal plasma cells: regulation during interleukin-6(IL-6)-induced growth and survival. *Eur. J. Haematol.* 69:76–89. <http://dx.doi.org/10.1034/j.1600-0609.2002.01549.x>
- Sprynski, A.C., D. Hose, L. Caillot, T. Réme, J.D. Shaughnessy Jr., B. Barlogie, A. Seckinger, J. Moreaux, M. Hundemer, M. Jourdan, et al. 2009. The role of IGF-1 as a major growth factor for myeloma cell lines and the prognostic relevance of the expression of its receptor. *Blood.* 113:4614–4626. <http://dx.doi.org/10.1182/blood-2008-07-170464>
- Strobeck, M. 2007. Multiple myeloma therapies. *Nat. Rev. Drug Discov.* 6:181–182. <http://dx.doi.org/10.1038/nrd2269>
- Tu, Y., S. Renner, F. Xu, A. Fleishman, J. Taylor, J. Weisz, R. Vescio, M. Rettig, J. Berenson, S. Krajewski, et al. 1998. BCL-X expression in multiple myeloma: possible indicator of chemoresistance. *Cancer Res.* 58:256–262.
- van de Kooij, B., R.W. Rooswinkel, F. Kok, M. Herrebout, E. de Vries, M. Paauwe, G.M. Janssen, P.A. van Veelen, and J. Borst. 2013. Polyubiquitination and proteasomal turnover controls the anti-apoptotic activity of Bcl-B. *Oncogene.* 32:5439–5448. <http://dx.doi.org/10.1038/onc.2013.99>
- Wuillème-Toumi, S., N. Robillard, P. Gomez, P. Moreau, S. Le Gouill, H. Avet-Loiseau, J.L. Harousseau, M. Amiot, and R. Bataille. 2005. Mcl-1 is overexpressed in multiple myeloma and associated with relapse and shorter survival. *Leukemia.* 19:1248–1252. <http://dx.doi.org/10.1038/sj.leu.2403784>
- Zhai, D., N. Ke, H. Zhang, U. Lador, M. Joseph, A. Eichinger, A. Godzik, S.C. Ng, and J.C. Reed. 2003. Characterization of the anti-apoptotic mechanism of Bcl-B. *Biochem. J.* 376:229–236. <http://dx.doi.org/10.1042/bj20030374>
- Zhou, P., N.B. Levy, H. Xie, L. Qian, C.Y. Lee, R.D. Gascoyne, and R.W. Craig. 2001. MCL1 transgenic mice exhibit a high incidence of B-cell lymphoma manifested as a spectrum of histologic subtypes. *Blood.* 97:3902–3909. <http://dx.doi.org/10.1182/blood.V97.12.3902>